

---

## Electronic Supplementary Information (ESI)

### **Towards efficient blue emission cationic Ir(III) complex with azole-type ancillary ligands: a joint theoretical and experimental study**

Shao-Fen Huang, Hai-Zhu Sun, Guo-Gang Shan\*, Yong Wu, Min Zhang\* and Zhong-Min Su\*

Institute of Functional Material Chemistry, faculty of chemistry, Northeast Normal University

Jilin 130024, People's Republic of China.

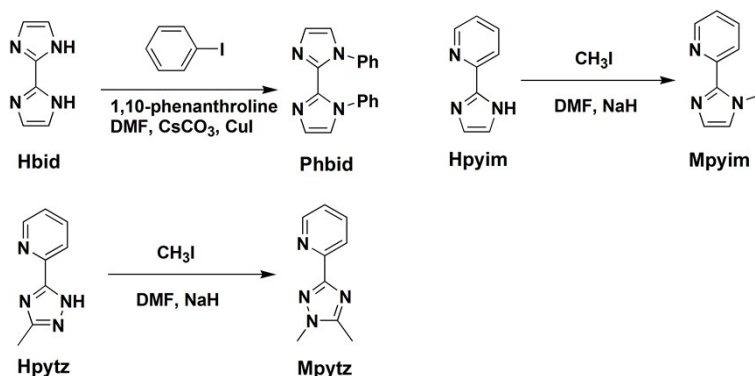
E-mail: [shangg187@nenu.edu.cn](mailto:shangg187@nenu.edu.cn) (G. G. Shan), [mzhang@nenu.edu.cn](mailto:mzhang@nenu.edu.cn) (M. Zhang), [zmsu@nenu.edu.cn](mailto:zmsu@nenu.edu.cn) (Z. M. Su)

#### **Table of Contents**

1. Synthesis and Characterization of the ligands used in this work	S2
2. Crystal data and structure refinements for complexes <b>1–4</b>	S3–S4
3. Photoluminescent spectra of complexes <b>1–4</b> at 77 K	S4
4. Calculated data	S5–S8
5. Cyclic voltammograms	S8

## Synthesis of ligands.

The precursors Hbid, Hpyim and Hpytz of ligands and ligand bpyim were readily synthesized according to early reported literature. All reactions were carried out under nitrogen protection.



**Scheme S1.** The synthetic routes of ancillary ligands Phbid, Mpyim and Mpytz.

### Phbid

A mixture of Hbid (0.54 g, 4 mmol), iodobenzene (2.04 g, 10 mmol), phenanthroline (0.84 g, 4 mmol), CsCO<sub>3</sub> (3.30 g, 10 mmol) and CuI (0.40 g, 2 mmol) in DMF (30 mL) was heated to reflux for 24 h. Solvent was removed by distillation under reduced pressure. The resulted residue was extracted by CH<sub>2</sub>Cl<sub>2</sub> and organic layer was dried by anhydrous Na<sub>2</sub>SO<sub>4</sub>. The further purification was performed by silica gel column chromatography using ethyl acetate as eluent to afford ligand **Phbid** (54.5%). <sup>1</sup>H NMR (CDCl<sub>3</sub>, 500 MHz)  $\delta$  (ppm): 7.26 (d,  $J$  = 1.5 Hz, 2H), 7.22–7.17 (m, 2H), 7.15–7.14 (m, 4H), 7.06 (d,  $J$  = 1.0 Hz, 2H), 6.72–6.70 (m, 4H).

### Mpyim

Hpyim (0.98 g, 4 mmol) and NaH (0.40 g, 16 mmol) were dissolved in DMF (10 mL) and stirred at room temperature for 1 h, followed by addition of CH<sub>3</sub>I (0.86 g, 6 mmol) dropwise. The reaction mixture was stirred at room temperature for 24 h. After reaction 30 mL of water was added. Then the solution was extracted with dichloromethane (20 mL) for three times. The organic layers were collected and dried with anhydrous Na<sub>2</sub>SO<sub>4</sub>. The further purification was performed by silica gel column chromatography using ethyl acetate and CH<sub>2</sub>Cl<sub>2</sub> as eluent to afford ligand **Mpyim** (50.3%). <sup>1</sup>H NMR (CDCl<sub>3</sub>, 500 MHz)  $\delta$  (ppm): 8.57 (d,  $J$  = 4.5 Hz, 1H), 8.17 (d,  $J$  = 8.0 Hz, 1H), 7.76–7.72 (m, 1H),

7.21–7.19 (m, 1H), 7.11 (s, 1H), 6.96 (s, 1H), 4.11 (s, 1H).

### Mpytz

Hpytz (0.64 g, 4mmol) and NaH (0.40 g, 16 mmol) were dissolved in DMF (10 mL) and stirred at room temperature for 1 h. Then CH<sub>3</sub>I (0.86 g, 3 mmol) was added dropwise under vigorously stir. After reaction 30 mL of water was added. Then the solution was extracted with CH<sub>2</sub>Cl<sub>2</sub> (20 mL) for three times. The organic layers were collected and dried with anhydrous Na<sub>2</sub>SO<sub>4</sub>. The further purification was performed by silica gel column chromatography using petroleum ether : ethyl acetate 3:1 then changed to CH<sub>2</sub>Cl<sub>2</sub> : CH<sub>3</sub>OH as eluent to afford ligand **Mpytz** (44.5%). <sup>1</sup>H NMR (CDCl<sub>3</sub>, 500 MHz) δ (ppm): 8.71 (d, *J* = 4.5 Hz, 1H), 8.06 (d, *J* = 8.0 Hz, 1H), 7.78–7.75 (m, 1H), 7.30–7.27 (m, 1H), 3.90 (s, 3H), 2.53 (s, 3H).

**Table S1.** Crystal data and structure refinements for complexes **1**, **2** and **4**.

Complex	1	2	4
Formula	C <sub>74</sub> H <sub>54</sub> F <sub>20</sub> Ir <sub>2</sub> N <sub>16</sub> O <sub>2</sub> P <sub>2</sub>	C <sub>32</sub> H <sub>21</sub> F <sub>10</sub> IrN <sub>7</sub> P	C <sub>41</sub> H <sub>41</sub> O <sub>4</sub> F <sub>10</sub> Ir N <sub>8</sub> PCl <sub>2</sub>
Formula weight	2025.67	916.73	997.07
Crystal system	Monoclinic	Monoclinic	Triclinic
Space group	C2/c	P21/n	P-1
<i>a</i> /Å	22.115(5)	9.8440(4)	11.2530(8)
<i>b</i> /Å	17.117(5)	24.2180(11)	11.5830(8)
<i>c</i> /Å	23.322(5)	15.7880(7)	15.2630(11)
<i>α</i> /°	90	90	103.2960(13)
<i>β</i> /°	109.896(3)	101.8570(14)	99.1430(15)
<i>γ</i> /°	90	90	109.7520(14)
<i>V</i> /Å <sup>3</sup>	8301(3)	3683.6(3)	1760.3(2)
<i>Z</i>	4	4	2
Density(calculated)/Mg m <sup>-3</sup>	1.621	1.653	1.881
Absorption coefficient /mm <sup>-1</sup>	3.340	3.751	4.154
F(000)	3960	1776	966

Observed reflection/unique	23708 / 8837	64548 / 7277	10207/ 6197
$R_{int}$	0.0582	0.0774	0.0386
Goodness-of-fit on $F^2$	1.028	1.078	1.041
$R_1^a$ , $wR_2^b$ [ $I > 2\sigma(I)$ ]	0.0499, 0.1503	0.0819, 0.2399	0.0419, 0.0830
$R_1$ , $wR_2$ (all data)	0.0953, 0.1746	0.1022, 0.2680	0.0616, 0.0908

$^a R_1 = \Sigma ||F_o| - |F_c|| / \Sigma |F_o|$ .  $^b wR_2 = [\Sigma w(|F_o| - |F_c|)^2] / \Sigma w(F_o)^2)^{1/2}$ .

**Table S2.** Selected bond distances and angles for complexes **1**, **2** and **4**.

Complex	<b>1</b>	<b>2</b>	<b>4</b>
Ir–C <sub>C^N</sub>	2.007(9)	2.023(11)	2.000(2)
	2.014(9)	2.018(12)	2.020(3)
Ir–N <sub>C^N</sub>	2.018(8)	2.029(10)	2.016(2)
	2.026(8)	2.037(11)	2.026(2)
Ir–N <sub>N^N</sub>	2.138(7)	2.112(10)	2.153(2)
	2.141(7)	2.160(10)	2.161(2)
N <sub>C^N</sub> –Ir–N <sub>C^N</sub>	172.0(3)	172.7(4)	172.80(9)
C <sub>C^N</sub> –Ir–N <sub>C^N</sub>	80.7(4)	81.0(5)	80.53(9)
	80.3(3)	80.4(5)	79.74(10)
N <sub>N^N</sub> –Ir–N <sub>N^N</sub>	76.2(3)	76.0(4)	75.37(8)

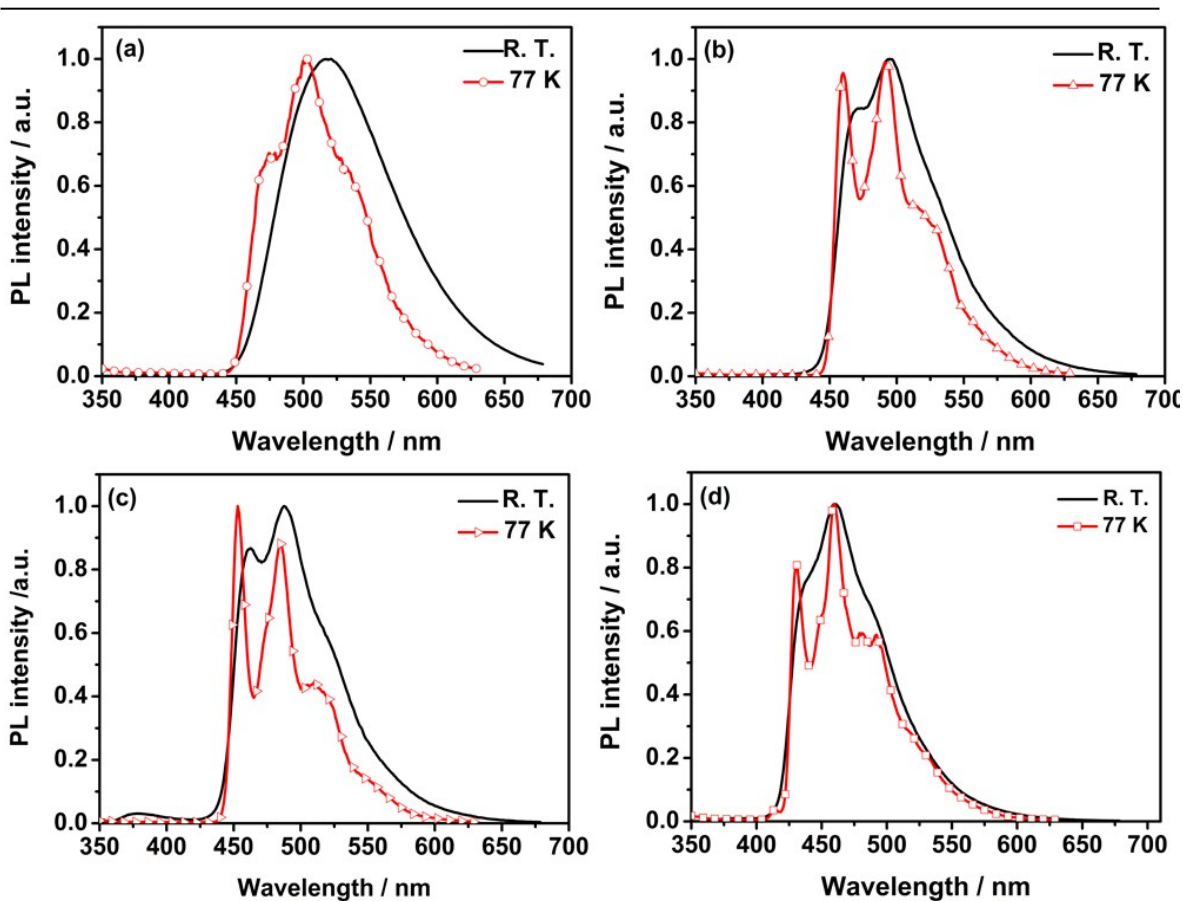
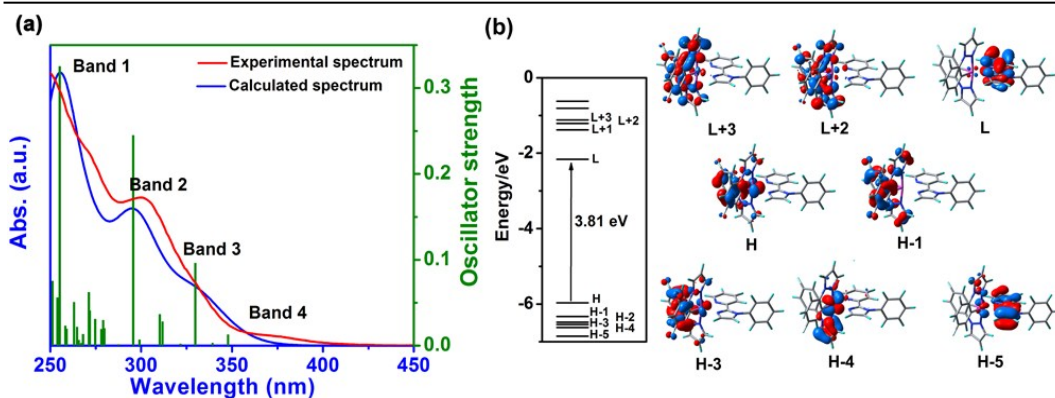


Fig. S1. Photoluminescent spectra of complexes 1–4 at room temperature and 77 K.

Table S3. Calculated excited energies, dominant orbital excitations, and oscillator strength ( $f$ ) of complex 2 in CH<sub>3</sub>CN solution from TD-DFT calculation.

2	Excited state	eV/nm	$f$	Major contributions <sup>a</sup>	Character <sup>b</sup>
Band 1	S26	4.86/255	0.32	H-3→L+2 (24%)	IL
				H-4→L+3 (14%)	IL/LLCT/MLCT
				H-1→L+3 (15%)	IL
Band 2	S9	4.19/296	0.24	H-5→L (84%)	IL
Band 3	S4	3.76/330	0.01	H-4→L (88%)	LLCT/MLCT
Band 4	S1	3.14/394	0.0001	H→L (98%)	MLCT/LLCT

<sup>a</sup> H and L denote HOMO and LUMO, respectively. <sup>b</sup> MLCT, LLCT and IL denote metal-to-ligand charge transfer, ligand-to-ligand and ligand centered charge transfer, respectively.



**Fig. S2.** (a) TD-DFT simulated and experimental absorption spectra of complex **2** in  $\text{CH}_3\text{CN}$ . (b) The shape of frontier electronic levels and selected frontier molecular orbitals involved in crucial electronic excitations of complexes **2**. H and L denote HOMO and LUMO, respectively.

**Table S4.** Calculated excited energies, dominant orbital excitations, and oscillator strength ( $f$ ) of complex **3** in  $\text{CH}_3\text{CN}$  solution from TD-DFT calculation.

<b>3</b>	Excited state	eV/nm	$f$	Major contributions <sup>a</sup>	Character <sup>b</sup>
Band 1	S23	4.85/255	0.32	H-4→L+3 (14%)	IL/MLCT
				H-3→L+2 (24%)	IL/MLCT
				H-1→L+3 (16%)	IL
Band 2	S9	4.17/297	0.22	H-5→L (81%)	IL
Band 3	S4	3.77/329	0.09	H-4→L (87%)	LLCT/MLCT
Band 4	S2	3.57/348	0.01	H-2→L (91%)	LLCT/MLCT/IL
	S1	3.15/394	0	H→L (98%)	MLCT/LLCT

<sup>a</sup> H and L denote HOMO and LUMO, respectively. <sup>b</sup> MLCT, LLCT and IL denote metal-to-ligand charge transfer, ligand-to-ligand and ligand centered charge transfer, respectively.

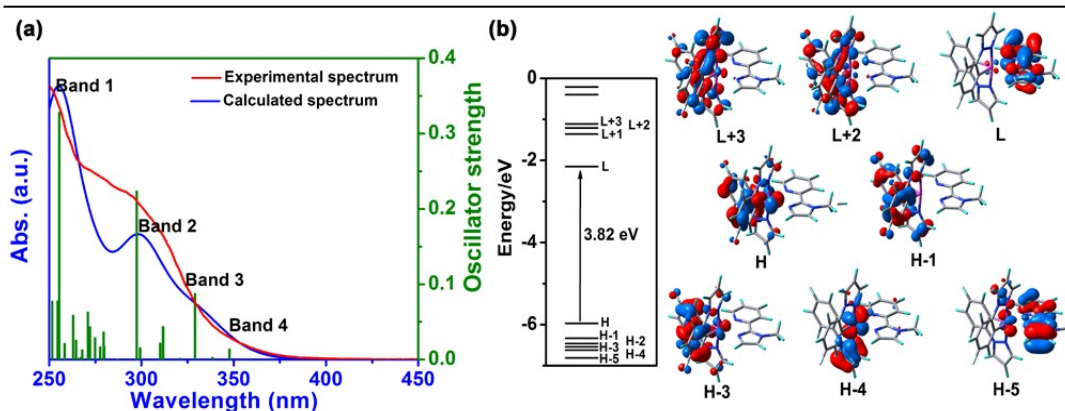


**Fig. S3.** TD-DFT simulated and experimental absorption spectra of complex **3** in CH<sub>3</sub>CN. (b) The shape of frontier electronic levels and selected frontier molecular orbitals involved in crucial electronic excitations of complexes **3**. H and L denote HOMO and LUMO, respectively.

**Table S5.** Calculated excited energies, dominant orbital excitations, and oscillator strength (*f*) of complex **4** in CH<sub>3</sub>CN solution from TD-DFT calculation.

<b>4</b>	Excited state	eV/nm	<i>f</i>	Major contributions <sup>a</sup>	Character <sup>b</sup>
Band 1	S23	4.85/256	0.38	H-3→L+2 (16%) H-1→L+3 (18%) H-4→L+3 (11%)	LLCT/MLCT IL IL/LLCT/MLCT
Band 2	S4	3.86/321	0.09	H-4→L (88%)	MLCT/LLCT
Band 3	S2	3.66/338	0.001	H-2→L (73%) H-3→L (20%)	MLCT/LLCT MLCT/LLCT
	S1	3.26/380	0	H→L (97%)	MLCT/LLCT

<sup>a</sup> H and L denote HOMO and LUMO, respectively. <sup>b</sup> MLCT, LLCT and IL denote metal-to-ligand charge transfer, ligand-to-ligand and ligand centered charge transfer, respectively.

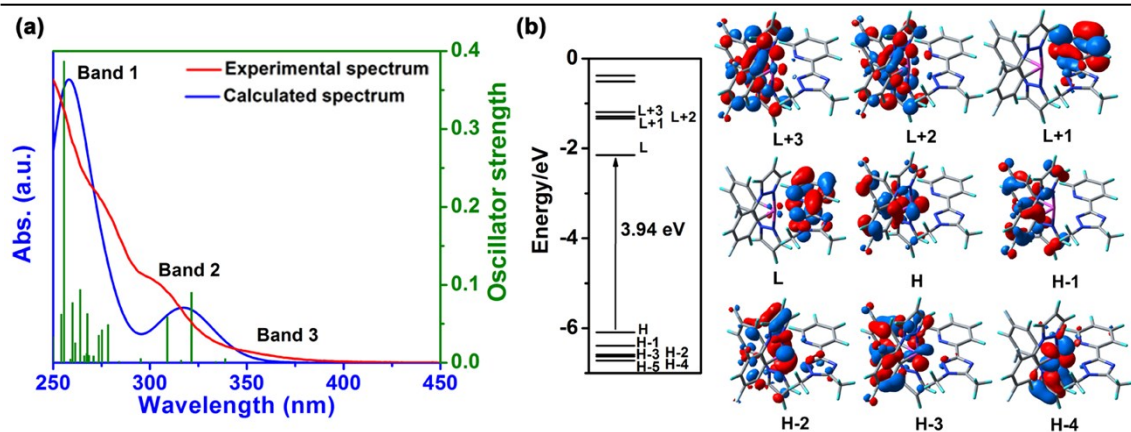


**Fig. S4.** TD-DFT simulated and experimental absorption spectra of complex **4** in  $\text{CH}_3\text{CN}$ . (b) The shape of frontier electronic levels and selected frontier molecular orbitals involved in crucial electronic excitations of complexes **4**. H and L denote HOMO and LUMO, respectively.

**Table S6.** Calculated triplet states of complexes **1–4** by a TD-DFT approach.

Complex	State	eV	$f$	Assignment <sup>a</sup>	Character <sup>b</sup>
<b>1</b>	$T_1$	2.01	0.00	H-1 $\rightarrow$ L (58%)	$^3\text{MLCT}/^3\text{LLCT}$
				H $\rightarrow$ L (38%)	$^3\text{MLCT}/^3\text{LLCT}$
<b>2</b>	$T_1$	2.30	0.00	H-2 $\rightarrow$ L (73%)	$^3\text{MLCT}/^3\text{LLCT}/^3\text{LC}$
				H-5 $\rightarrow$ L (12%)	$^3\text{LC}$
<b>3</b>	$T_1$	2.38	0.00	H-2 $\rightarrow$ L (71%)	$^3\text{MLCT}/^3\text{LLCT}/^3\text{LC}$
				H-5 $\rightarrow$ L (14%)	$^3\text{LC}$
<b>4</b>	$T_1$	2.69	0.00	H $\rightarrow$ L+1 (86%)	$^3\text{MLCT}/^3\text{LC}$

<sup>a</sup>H and L denote HOMO and LUMO, respectively. <sup>b</sup>MLCT, LLCT and LC denote metal-to-ligand charge transfer, ligand-to-ligand and ligand centered charge transfer, respectively.



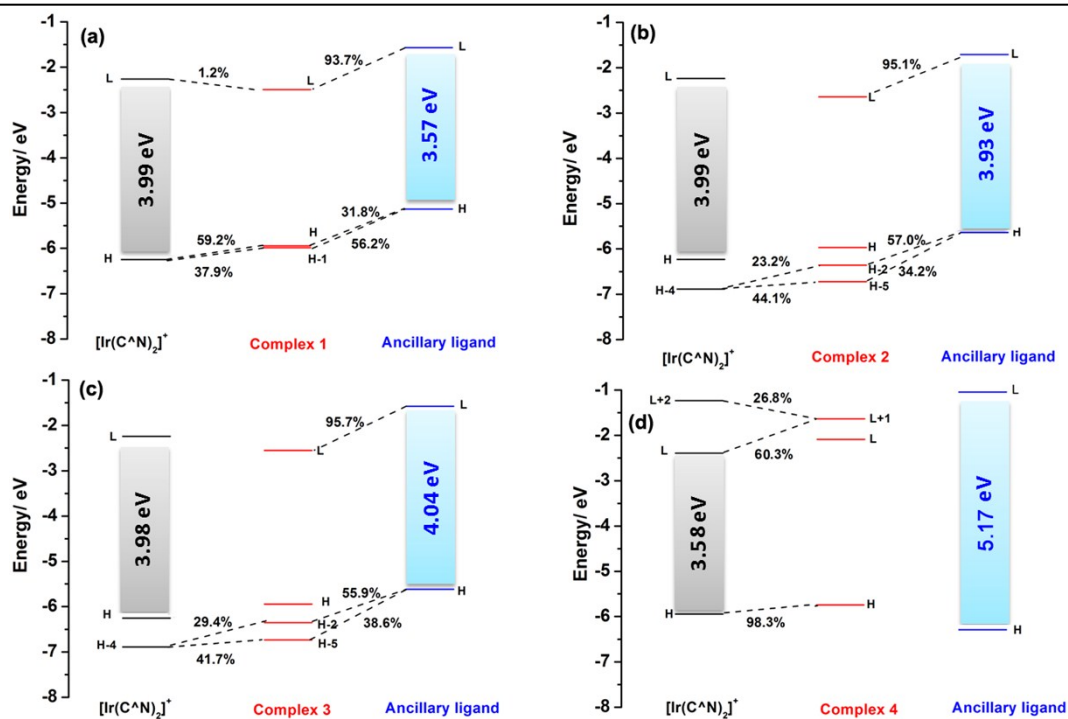


Fig. S5. Molecular orbital correlation diagrams for complexes 1–4.

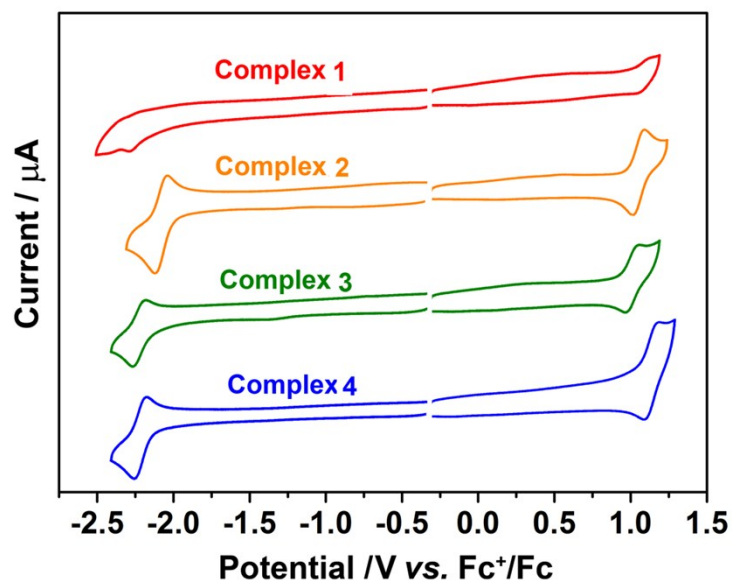


Fig. S6. Cyclic voltammograms of the cationic Ir(III) complexes 1–4 in  $\text{CH}_3\text{CN}$  solutions. Potentials were recorded versus  $\text{Fc}^+/\text{Fc}$  (Fc is ferrocene).